

We are IntechOpen, the world's leading publisher of Open Access books Built by scientists, for scientists

6,900

Open access books available

185,000

International authors and editors

200M

Downloads

Our authors are among the

154

Countries delivered to

TOP 1%

most cited scientists

12.2%

Contributors from top 500 universities



WEB OF SCIENCE™

Selection of our books indexed in the Book Citation Index
in Web of Science™ Core Collection (BKCI)

Interested in publishing with us?
Contact book.department@intechopen.com

Numbers displayed above are based on latest data collected.
For more information visit www.intechopen.com



Septocutaneous Gluteal Artery Perforator (Sc-GAP) Flap for Breast Reconstruction: How We Do It

Stefania Tuinder, Rene Van Der Hulst, Marc Lobbes,
Bas Versluis and Arno Lataster

Additional information is available at the end of the chapter

<http://dx.doi.org/10.5772/56224>

1. Introduction

In 1976 the first free flap for breast reconstruction was reported by Fujino: he used the gluteus maximus myocutaneous flap. A skin-fat-muscle flap, including the superior gluteal artery and veins, was dissected and anastomosed to the thoracoacromial artery and vein [1]. In 1983 Shaw published a series of 10 patients undergoing the superior gluteal myocutaneous free flap [2]: technical refinements were added to the work of Fujino. Only in 1993 Allen introduced the superior gluteal artery perforator (S-GAP) flap for breast reconstruction [3]. The pedicle of the flap was longer than that of the gluteus maximus myocutaneous flap because of the intramuscular dissection: as a consequence a vein graft was not necessary to perform the micro-anastomosis: moreover no muscle was sacrificed giving less donor site morbidity. In 2010 LoTempio and Allen published a review of the latest 17 years with gluteal flaps [4]: over the years the donor site is just improved, positioning the scar in the upper buttock superior from medial to lateral and beveling superior to reduce the contour deformity. Their experience showed a complication rate of 2 % of flap loss. The improvement in technique and results is also due to the introduction of new technologies such as MRA (magnetic resonance angiography) and CTA (computed tomography angiography) supporting the identification of the best perforator.

Within the first years of development of perforator flaps confusion arose about the nomenclature: for example the flap based on paraumbilical perforators, originating from the deep inferior epigastric artery, was called PUP (paraumbilical perforator flap) by Koshima [5] and DIEP (deep inferior epigastric perforator) flap by Allen and Treece [6]. Attempts were made to unify the perforator flap nomenclature:

1. In 2001, during the fifth international course on perforator flaps in Gent, Belgium [7]
2. The Canadian proposal, summarized in an article by Geddes et al. [8].
3. The Asian microsurgical community proposal, with a tendency to use a more complex terminology [9].

Discussion however is still open regarding the nomenclature of perforator flaps and the last proposal is published in 2010 by Sinna et al. [10]. In 2012 Taylor commented that with the advent of modern imaging techniques, the true subcutaneous course of a perforator has to be considered in the classification and in the flap design [11].

Clinically it is really important to distinguish perforators running through the muscle (in this chapter indicated as musculocutaneous) and perforators running between two muscles (septocutaneous) because they have different clinical implications, particularly with respect to the S-GAP flap. The evolution from the S-GAP (superior gluteal artery perforator) flap to the Sc-GAP (septocutaneous gluteal artery perforator) flap reflects the above mentioned concept. We published a preliminary anatomical study [12] and later on a clinical study [13] on this concept showing that the use of septocutaneous perforators can make the dissection of the flap easier with an improvement in the aesthetic results of the donor site.

1.1. Topographical and functional anatomy of the gluteal region

This paragraph is partly based on Gray's Anatomy [14], Moore Clinically Oriented Anatomy [15] and Stone and Stone's Atlas of Skeletal Muscles [16].

The gluteal region or buttock is bounded cranially by the iliac crest and caudally by the oblique border of the gluteus maximus muscle. The horizontal skin fold of the buttock, indicated as gluteal fold (sulcus glutealis, ruga glutealis horizontalis), is often mistaken for this caudal border. It is important clinically to define the exact borders of the gluteal region in order to achieve skin projections of underlying bony landmarks, muscles, nerves and blood vessels as accurately as possible. The crena analis or crena ani is the vertical cleft, leading to the anus, between the left and right buttock. It is also called (crena) clunium, gluteal furrow, intergluteal or natal cleft, rima ani or rima clunium. Besides the iliac crest, the anterior superior iliac spine (ASIS) and the posterior superior iliac spine (PSIS), at the beginning and end of the iliac crest, are important bony landmarks. The PSIS is marked by a skin dimple. Caudomedially the ischial tuberosity can be palpated, deep to the gluteus maximus muscle. Laterally the greater trochanter is an important, palpable landmark. The prominence of the buttock is not only formed by the gluteus maximus muscle, but in the craniolateral part also by the gluteus medius.

In the gluteal region two muscle layers can be distinguished: (1) a superficial layer containing the gluteus maximus, and (2a-e) a deep layer containing the gluteus medius, gluteus minimus, piriformis, triceps coxae and quadratus femoris muscles (fig 1). The gluteus muscles are mainly extensors and abductors in the hip joint, the piriformis, triceps coxae and quadratus femoris are mainly lateral rotators.

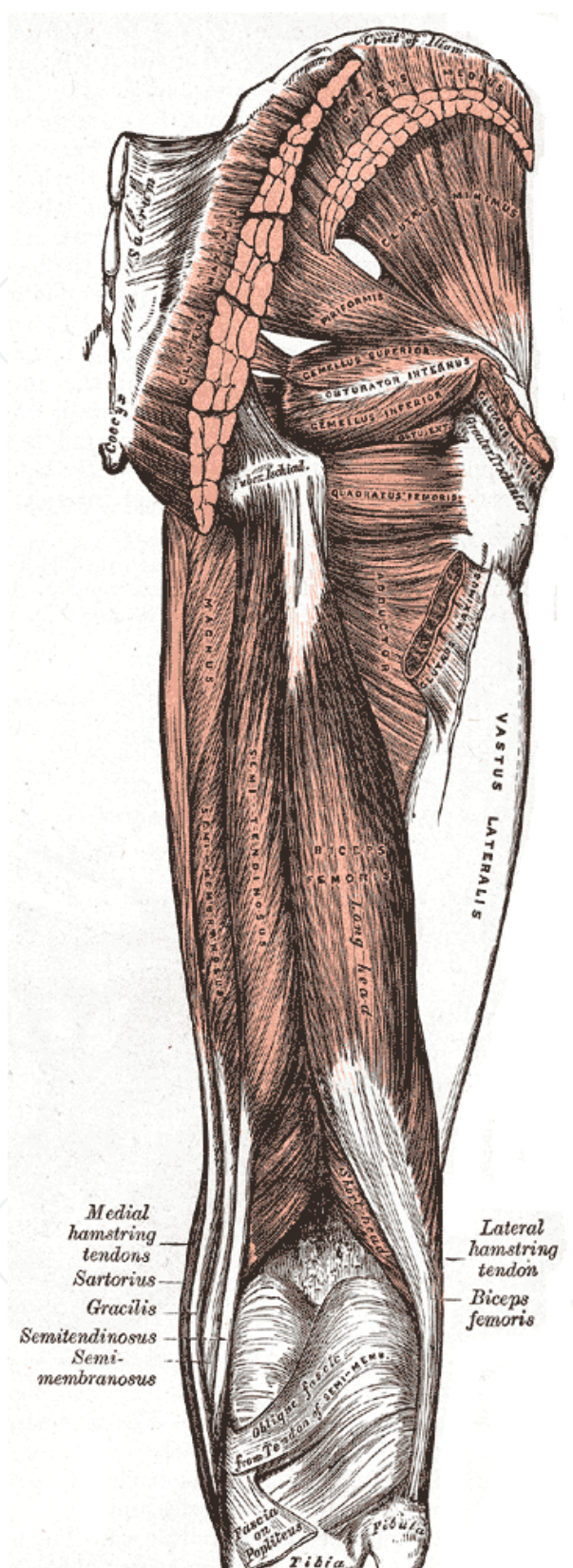


Figure 1. Muscles of the gluteal region and the posterior thigh.

(1) The gluteus maximus muscle is the largest, thickest and most superficial muscle in the buttock. It originates from the outer surface of the ilium, dorsally from the posterior gluteal line, from the adjacent dorsal surface of the lower sacrum and from the lateral coccyx. Connective tissue muscle origins are the sacrotuberal ligament, the erector spinae aponeurosis and the gluteus medius fascia. Muscle fibers descent obliquely and laterally, where the thicker and larger cranial part of the muscle merges with the superficial fibers of the caudal part to continue over the greater trochanter as the iliotibial tract, a reinforcement of the deep fascia lata of the thigh. The tensor fasciae latae muscle, originating from the outer edge of the iliac crest, between the ASIS and the iliac tubercle, also continues in the iliotibial tract, steadying the femur on the tibia during walking, in conjunction with the gluteus maximus muscle. When taking the fixed point at the pelvis, the cranial part of the gluteus maximus is active in abduction and lateral rotation of the thigh and the caudal part extends and also laterally rotates the thigh. When taking the fixed point distally, it stabilizes the trunk during bipedal gait and, together with the hamstrings, raises it.

(2a) The gluteus medius muscle is a broad, thick, fan-shaped muscle. It originates from the outer surface of the ilium caudal to the iliac crest and inserts at the lateral surface of the greater trochanter. Optionally a deep slip of muscle may be attached to the cranial end of it. The caudal part of the gluteus medius muscle is covered by the gluteus maximus, divided from it by a thin connective tissue septum, and bordered (and sometimes partly covered) by the piriformis muscle. The cranial part of the gluteus medius is covered by a strong deep gluteal fascia, on which the gluteus maximus muscle fibers attach caudally and the gluteus medius muscle fibers attach from the inner side. The craniomedial origin of the gluteus maximus doesn't reach the midline and is quite thin. More to the lateral side the muscle becomes thicker. Therefore it is easier to find an intermuscular septum between the gluteus maximus and medius muscles at a distance of about 7 cm from the midline. The gluteus medius is a strong abductor at the hip joint and important in stabilizing the pelvis: it is largely responsible for pelvic tilt during walking. The caudal part of the muscle, inserting more to the anterior of the greater trochanter, also medially rotates the thigh.

(2b) The gluteus minimus muscle is the smallest and thinnest of the gluteus muscles. Like the gluteus medius it is a fan-shaped, triangular muscle. It originates from the outer surface of the ilium, between the middle (anterior) and lower (inferior) gluteal lines and, behind, from the margin of the greater sciatic notch. The muscle fibers converge to an aponeurosis that is continuous with the cranial part of the triangular iliofemoral ligament. This aponeurosis finally, as a capsular expansion, inserts to the anterior surface of the greater trochanter. During locomotion the gluteus minimus exerts the same action as the gluteus medius. The anterior fibers medially rotate the thigh more strongly than the gluteus medius muscle.

The muscles described below (2c-e) are all located caudally and deeper than the region of surgical dissection of the Sc-GAP (see also 'Arterial topography') and are described to complete the muscular anatomy of the gluteal region.

(2c). Yet, the piriformis muscle is an important key-structure in the gluteal region to understanding innervation and vascularization (see below). This pear-shaped muscle arises from the internal (anterior) surface of the sacrum, leaving the lesser pelvis through the greater sciatic

foramen. It also originates from the region near the posterior inferior iliac spine (PIIS), the adjacent sacroiliac joint capsule and sometimes the inner (pelvic) part of the sacrotuberous ligament. Its insertion, often blended with that of the triceps coxae muscles, which are attaching more posteriorly and caudally, is on the cranial border of the greater trochanter. Sometimes the piriformis muscle belly is also blended with that of the gluteus medius. It laterally rotates the thigh at the hip joint and abducts the thigh.

(2d) The triceps coxae muscle is composed of the gemellus superior, obturator internus and gemellus inferior muscle.

(2e) The quadratus femoris muscle is a flat, rectangular muscle, located between the gemellus inferior and the cranial border of the adductor magnus.

1.2. Arterial topography of the gluteal region

The gluteal region is supplied by the superior and inferior gluteal arteries (SGA and IGA), both directly branching from the internal iliac artery. The accompanying venous tree shows a similar ramification pattern and finally drains into the internal iliac vein (fig 2).

1.3. The superior gluteal artery

The short and large superior gluteal artery (SGA) is a continuation of the posterior trunk of the internal iliac artery and runs posteriorly between the lumbosacral trunk and the first sacral ventral ramus. Within the lesser pelvis it supplies the piriformis and obturator internus muscles and is a nutrient artery for the hip bone. It leaves the greater sciatic foramen cranial to the piriformis muscle and immediately ramifies into (1) superficial and (2) deep branches (fig 3). The superficial branch of the SGA enters the septal plane between the gluteus medius and gluteus maximus muscles. From that plane there are three clinical important ramifications:

(1a) Muscular branches that only supply the gluteus maximus itself.

(1b) Septocutaneous perforators which reach the subcutis and skin, running through the interseptal plane between the gluteus maximus and medius muscles (fig 4).

(1c) Musculocutaneous perforators which finally reach the subcutis and skin, running through the gluteus maximus muscle.

The superficial branch of the SGA anastomizes with branches of the inferior gluteal artery (IGA), the medial circumflex femoral artery and the lateral sacral artery. Comark and Lamberty [17] also described a superficial branch using the septal connective tissue plane between the gluteus maximus and the gluteus medius to divide into a posterior, intermediate and anterior branch. Anterior end branches pierce the deep fascia in the superolateral edge of the gluteus maximus muscle to supply the (sub)cutis there (septocutaneous perforators, as mentioned above).

(2) The deep branch of the SGA runs between the gluteus medius muscle and the posterior pelvic surface (gluteus minimus and piriformis muscles). It divides into a (2a) superior and an (2b) inferior division.

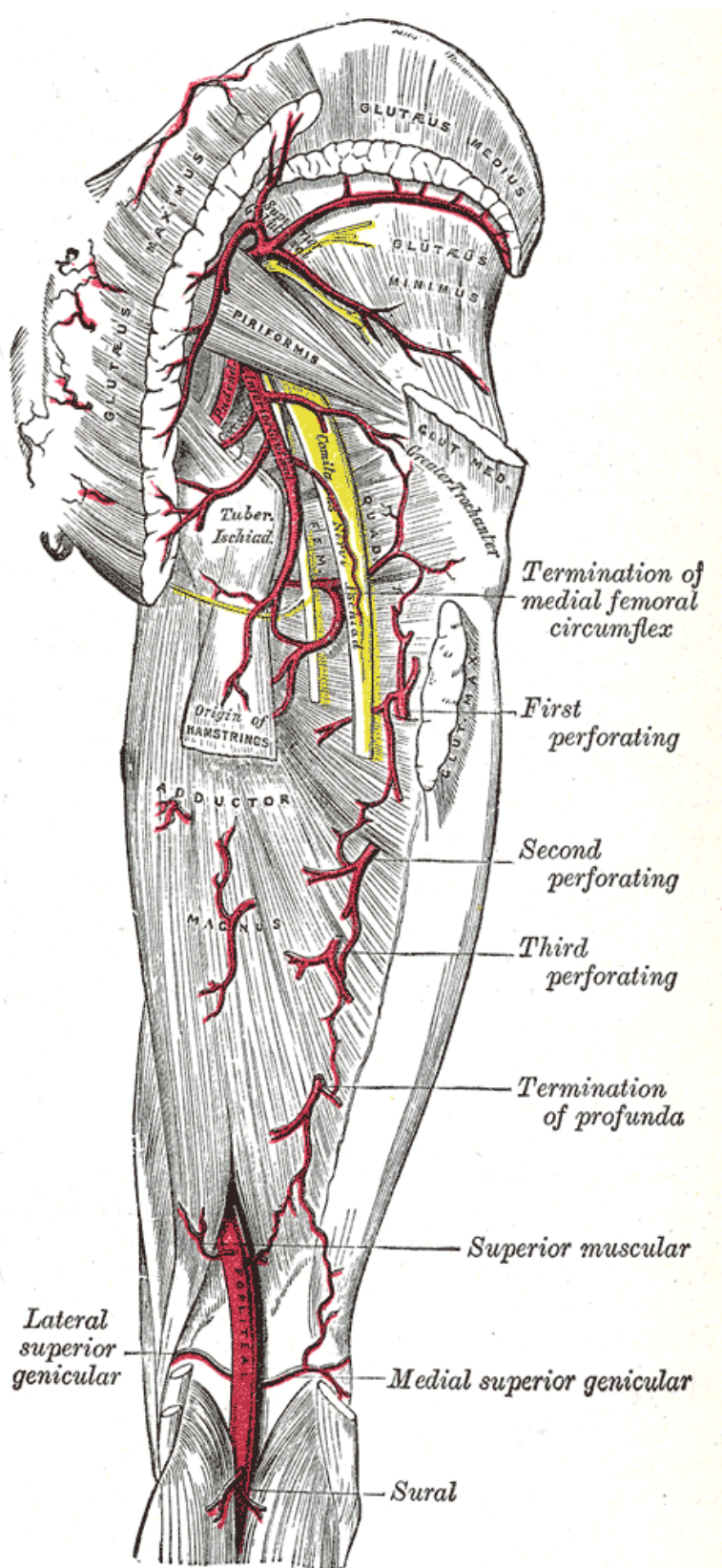


Figure 2. Arteries and nerves of the gluteal region and the posterior thigh.

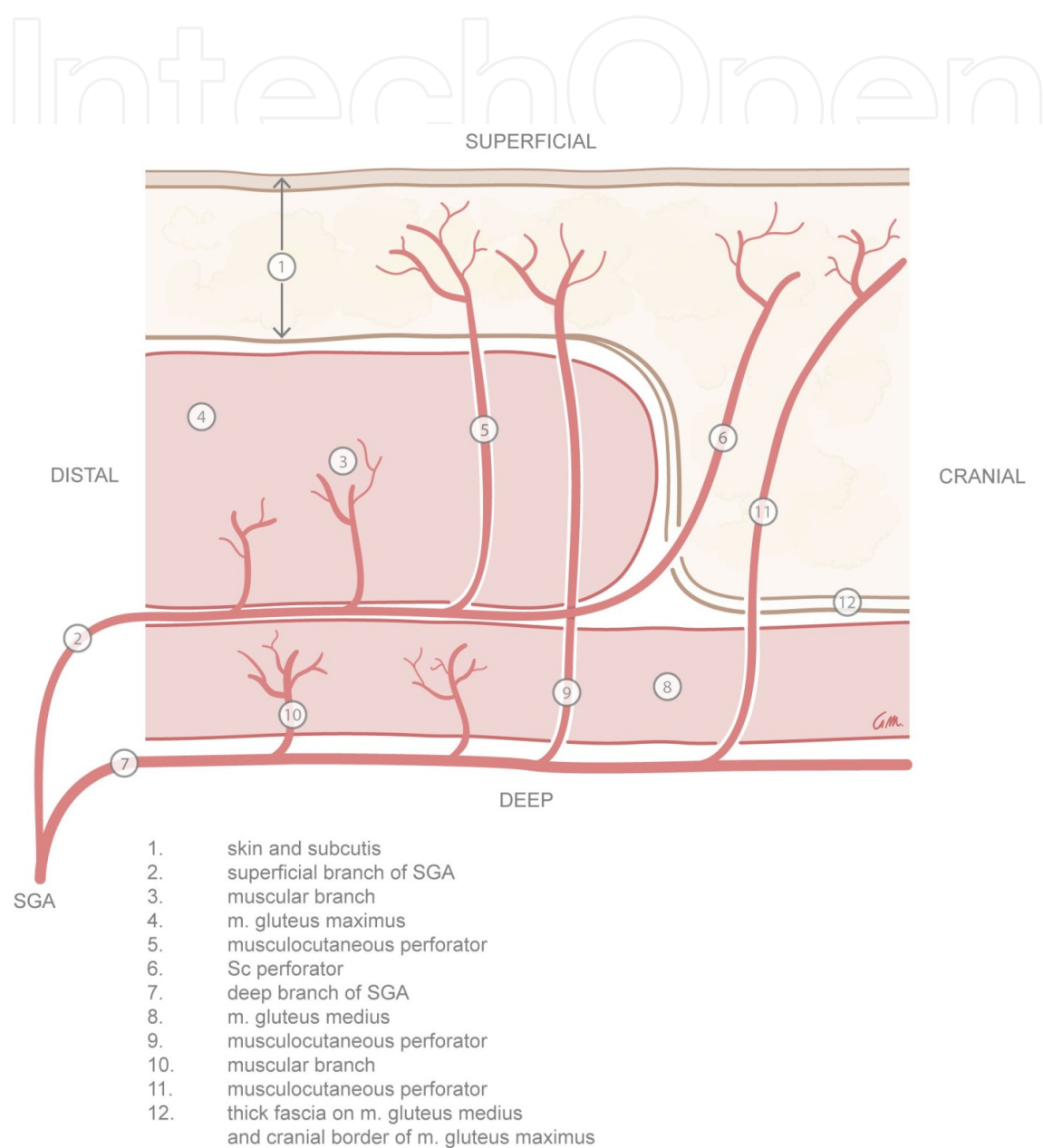


Figure 3. Schematic illustration of the course of perforators and muscular branches originating from the superficial and the deep branch of the superior gluteal artery. Illustration of Greet Mommen, www.greetmommen.be.



1. Sc perforator
2. Sc perforator
3. Sc perforator
4. fascia on m. gluteus medius
5. m. gluteus maximus

green ligations: gluteal perforators

Figure 4. Cadaveric dissection: musculus gluteus maximus partly detached from its origin to show the septocutaneous perforators underneath.

(2a) The superior division supplies the gluteus medius muscle, continues obliquely along the upper border of the gluteus minimus and supplies also the latter. Finally it runs along the ASIS and anastomizes with the deep circumflex iliac artery and the ascending branch of the lateral circumflex femoral artery.

(2b) The inferior division also runs obliquely between the gluteus medius and minimus muscles, supplies them both and, like the superior division, anastomizes with the lateral circumflex femoral artery. One branch of the inferior division, in the trochanteric fossa, joins the inferior gluteal artery (IGA) and the ascending branch of the medial circumflex artery. Other branches pierce the gluteus minimus muscle into the deep, to supply the hip joint. The deep branch also gives off musculocutaneous perforator, reaching the skin through gluteus medius and maximus muscles. Those branches have to be excluded as pedicle for the S-GAP, because of the difficult dissection through the two muscles.

At the point where the superficial and the deep branch of the SGA meet, near the opening cranial to the piriformis muscle, a venous network of large, fragile bloodvessels is present forming a caput medusae. Clinically the dissection always should stop before reaching this caput medusae.

1.4. The inferior gluteal artery

The inferior gluteal artery (IGA) is the larger terminal branch of the anterior trunk of the internal iliac artery. It descends anterior from the sacral plexus and the piriformis muscle, behind the internal pudendal artery. Inside the pelvis it supplies piriformis, pelvic floor, perianal fat and branches to the fundus of the bladder and to the seminal vesicles and the prostate. It leaves the greater sciatic foramen below the piriformis muscle, supplying gluteus maximus, obturator internus, gemelli, quadratus femoris and upper hamstrings. The extra-pelvic part of the IGA anastomoses with the SGA and with the internal pudendal, obturator and medial circumflex femoral arteries.

1.4.1. Nerves in the gluteal region

The gluteal region is innervated by many nerves that can be divided into a superficial and a deep group. The deep nerves are the most important clinically.

1.4.2. The superficial gluteal nerves

The skin of the buttock receives cutaneous nerves from several lumbar and sacral segments, called cluneal nerves. They are divided into a (1) superior, (2) middle and an (3) inferior cluneal group.

1.4.3. The deep gluteal nerves

The seven deep gluteal nerves are branches of the sacral plexus. They leave the lesser pelvis through the greater sciatic foramen caudal to the piriformis muscle, except for the superior gluteal nerve, emerging cranial to this muscle.

1.4.4. *The superior gluteal nerve*

The superior gluteal nerve arises from the dorsal branches of the ventral rami of L4-L5 and S1 and leaves the pelvis cranial to the piriformis muscle together with the SGA. It accompanies the deep branch of the SGA (see above) between the gluteus medius and minimus and divides into a superior branch that supplies the gluteus medius and an inferior branch that supplies the gluteus medius and minimus and the tensor fasciae latae muscles.

1.4.5. *The inferior gluteal nerve*

This nerve arises from the dorsal branches of the ventral rami of L5 and S1-S2 and leaves the pelvis caudal to the piriformis muscle, superficially from the sciatic nerve and laterally from the pudendal nerve and internal pudendal artery, that, together with the IGA, all issue through the same space.

1.4.6. *The sciatic nerve*

This largest nerve in the body, the main branch of the sacral plexus, is formed by the ventral rami of L4-L5 and S1-S3. It usually does not supply structures in the pelvis, but is a well palpable landmark in the gluteal region. It usually passes out of the pelvis to enter the gluteal region caudal to the piriformis muscle and consists of a medial tibial and a lateral common peroneal nerve.

1.4.7. *The posterior femoral cutaneous nerve*

This nerve, supplying a very large skin area, also gives rise to the inferior cluneal nerves. It arises from the dorsal branches of the ventral rami of S1-S2, supplying the skin of the inferior buttock, and the ventral branches of the ventral rami of S2-S3, supplying the skin of the perineum.

1.4.8. *The nerve to the quadratus femoris muscle*

This nerve arises from the anterior divisions of the ventral rami of L4-L5 and S1 and leaves the pelvis caudal to the piriformis muscle.

1.4.9. *The nerve to the obturator internus muscle*

This nerve, arising from the anterior divisions of the ventral rami of L5 and S1-S2, leaves the pelvis caudal to the piriformis muscle and medial to the sciatic nerve.

1.4.10. *The pudendal nerve*

The pudendal nerve, arising from the anterior divisions of the ventral rami of S2-S4, leaves the pelvis caudal to the piriformis muscle as the most medial nerve

2. Preoperative radiological imaging

Numerous radiological imaging modalities are available to identify perforator branches in advance, facilitating surgical planning and shortening operative time [18,23]. At this moment, the most widely applied modalities in the preoperative evaluation and planning of perforator flap procedures are Doppler ultrasound (DUS) and CT angiography (CTA) [18]. Both these imaging techniques are widely available and relatively inexpensive. CT allows for beautiful 3D reconstructions, showing location, size and course of the perforators with high accuracy. Both modalities come with some disadvantages though. Doppler is associated with long imaging times, low accuracy and high interobserver variability [18,24]. CTA, on the other hand, suffers from exposure to ionizing radiation, which is an important drawback in the often (relatively) young patients, especially as the ovaries are within the field of view [25,27].

Magnetic resonance angiography (MRA) might overcome these disadvantages. Several authors have recently demonstrated that MR angiography is suitable as preoperative imaging modality to evaluate the perforator branches of the DIEA en SGA [18-20-22-28,29]. Excellent soft-tissue contrast and the absence of ionizing radiation are important advantages of MRI. Disadvantages of MRI, however, include limited availability and relatively long acquisition times. For now, experience with contrast-enhanced MR angiography (CE-MRA) in the preoperative workup of patients undergoing DIEP or S-GAP flap procedures is still scarce. Although studies comparing MRA and CTA/DUS generally report excellent results for MRA, the diversity in applied MRA techniques is large. Spatial resolution, applied contrast media (conventional extracellular contrast agents versus blood pool contrast agents), field strength (1,5 Tesla versus 3 Tesla magnets) and the application and method of fat-suppression techniques differ between studies. These differences, combined with the fact that most studies included only limited numbers of patients, make it difficult to determine the most optimal MRA protocol. In general, a higher spatial resolution will improve the sensitivity for detecting perforator branches at the cost of longer acquisition times and lower image quality (increased noise-levels). Blood pool contrast agents can be used for steady-state imaging to acquire high-resolution images with excellent signal-to-noise ratios. However, these agents suffer from limited availability and are relatively expensive compared to conventional extracellular contrast agents. Acquisition times are longer compared to first-pass imaging sequences using conventional contrast agents.

Higher field strength generally provides better signal-to-noise ratios and improved image quality. MRI scanners with field strengths of 3 Tesla or above are less widely available than 1.5 Tesla scanners. In addition, homogenous fat suppression is much more difficult to obtain at higher field strengths, which could result in unwanted image artifacts or decrease in vessel-to-background contrast ratios, as the perforator branches are located within the subcutaneous abdominal fat. To optimize contrast between the perforator branches and surrounding fat tissue, fat suppression can be very useful. Fat suppression requires a homogenous magnetic field, and is negatively influenced by patient movement (breathing and bowel movements), resulting in longer acquisition times. Given these variables, the most suitable MRA sequence to evaluate the perforator branches for each institution will depend on the local availability of MRI hardware, contrast agents and the allowed acquisition time.

As an example, the imaging in our institution is in general performed using 15 mL gadobutrol 1.0 mmol/mL (Gadovist®, Bayer Healthcare Pharmaceuticals), administered through the antecubital vein. An automatic injector is used, ensuring a constant flow rate of 1.5 mL/sec, followed by a saline flush. The field strength of our scanner is 1.5 Tesla and a four-channel SENSE body coil is used for imaging.

After the necessary survey and reference scans, we perform several sequences which are listed below. The sequence parameters of the sequences used in our hospital are also provided. Although these might differ between vendors and field strengths, we think they can serve as a basis for introducing this kind of MR imaging in the reader's own department.

Firstly, the transverse, balanced, T1-weighted FFE is performed, which has a field-of-view of 400x400 mm, and a slice thickness of 6 mm. Voxel size is 1.32 x 1.32 mm. Remaining scan parameters for this sequence are: TE 1.80 ms, TR 3.6 ms, flip angle 65 degrees (fig 5).

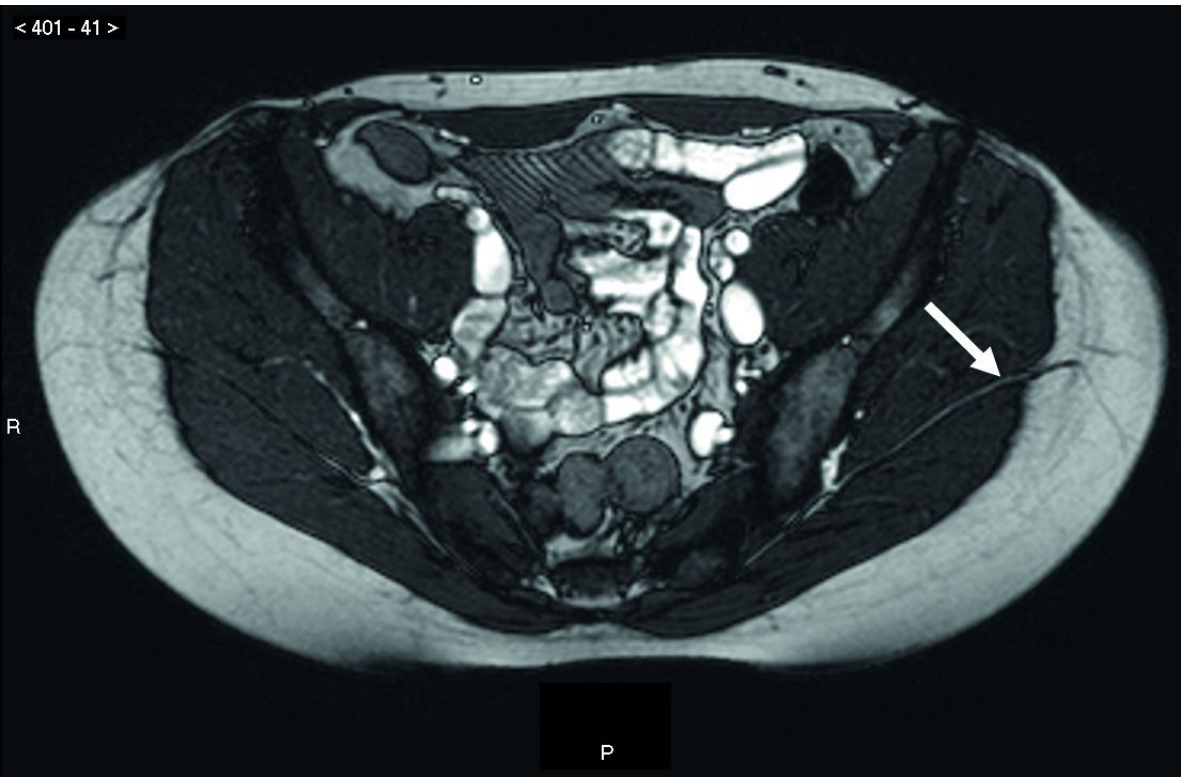


Figure 5. Transverse, balanced, T1-weighted FFE sequence on MRA. The arrow shows the perforator vein(s) running between gluteus maximus and medius muscle.

This is followed by a sagittal, balanced, T1-weighted fast field echo (FFE) is performed with a field-of-view 430x430 mm, and a slice thickness of 10 mm. Voxel size is 1.68 x 1.68 mm. The remaining scan parameters are: TE 1.56 ms, TR 3.1 ms, flip angle 65 degrees.

Next, a bolus tracker sequence is performed to assess the optimal time period of enhancement of the vessels of interest. This is followed by a coronal, three-dimensional T1-weighted FFE sequence, which has a field-of-view of 400x360 mm and a slice thickness of 2 mm. Voxel size is 1.0x1.36 mm. The remaining scan parameters are: TE 1.53 ms, TR 5.0 ms, flip angle 40 degrees.

Finally, a transverse, three-dimensional T1-weighted FFE sequence ('THRIVE') is acquired, which has a field-of-view of 380x304 mm and a slice thickness of 3 mm. Voxel size is 0.95x0.95 mm. The remaining scan parameters are: TE 3.9 ms, TR 7.8 ms, flip angle 10 degrees (fig 6).

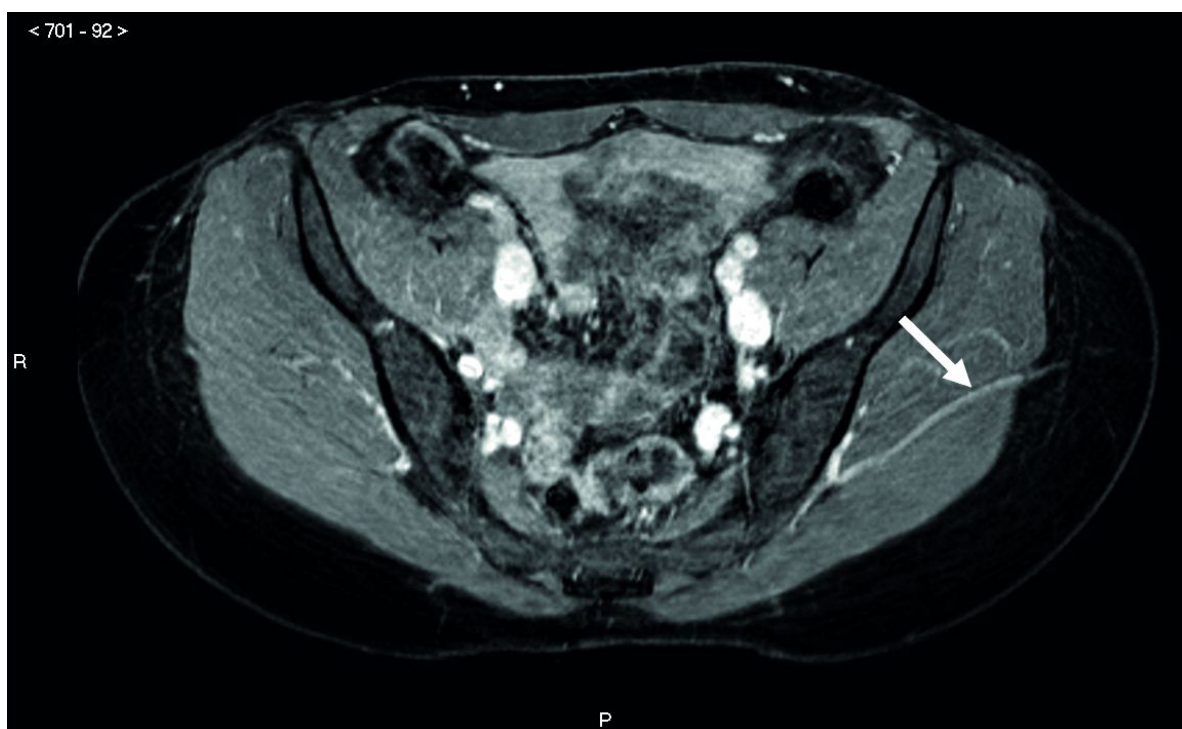


Figure 6. Transverse, three-dimensional T1-weighted FFE sequence ('THRIVE') on MRA. The arrow shows the comitant perforator artery running between gluteus maximus and medius muscle.

3. Preoperative landmarks

Step 1: Every patient undergoes preoperative imaging before surgery. Only patients with a suitable septocutaneous perforator are scheduled for breast reconstruction with Sc-GAP (75%). In MRA a septocutaneous perforator is considered suitable for surgery if the pedicle length is 6 cm or more.

Step 2: On the MRA the projection of the septocutaneous perforator on the surface of the patient is identified: because the gluteal region is not flat (as for example is the abdominal region) the

distance of the perforator from the midline is calculated on the curvature of the gluteal region (x axis) (fig 7).

The projection of the umbilicus on the patient's dorsal midline is identified as a landmark to determine the craniocaudal position of the perforator itself (y axis) (fig 8, A,B,C).

Step 3: To determine the position of the perforator as accurately as possible, a number of lines is drawn on the patient's skin. The patient's position should be the same as in surgery (see pitfalls). The midline is indicated with line A and the cranial end of the crena analis with a horizontal line B. With a color doppler (Esaote MyLab 25 Color Doppler with a LA523, 4-13 MHz probe) the cranial margin of the gluteus maximus muscle, where it originates from the thick gluteus medius fascia, is also identified, positioning the probe approximately parallel to this margin (fig 9A). It is marked on the skin as line C. Finally the iliac crest is identified and marked on the skin as a curved line D. The probe then is rotated 90° (fig 9B) and every perforator is identified and drawn on the skin: it is possible to identify perforators emerging from the septal plane between the gluteus maximus and medius muscles, though it is not possible to follow them to their origin from the SGA (fig 10).

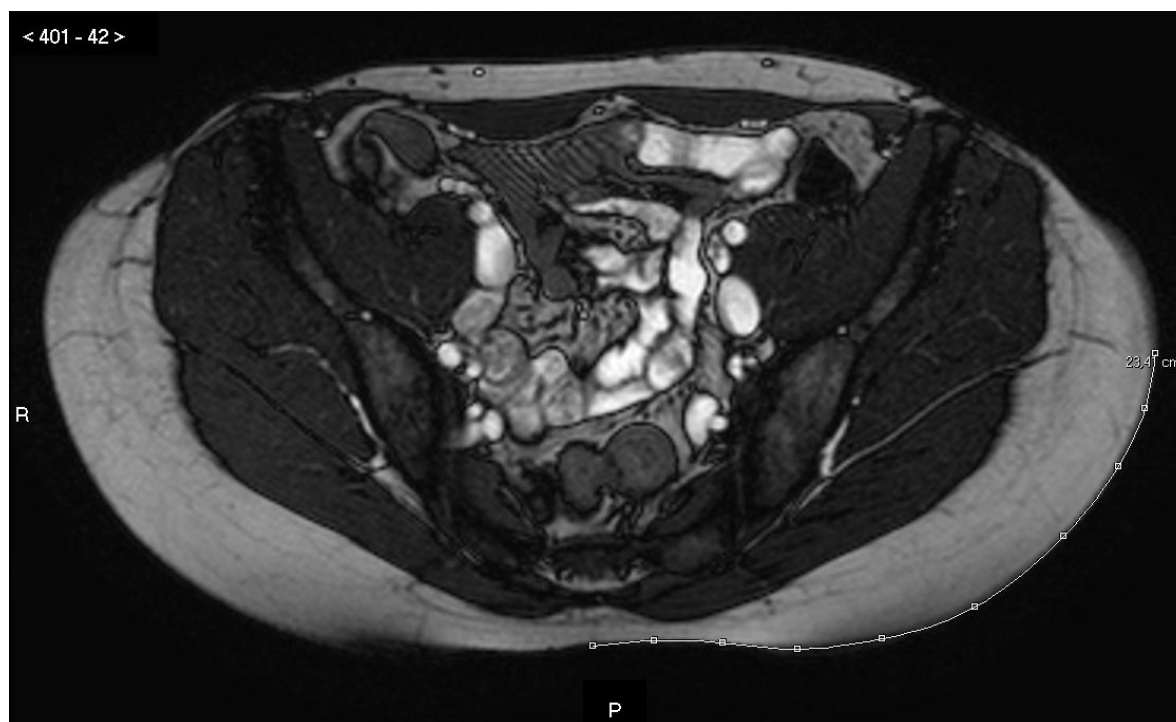


Figure 7. MRA imaging showing the measurement of the distance from the midline to the skin projection of the perforator chosen as pedicle for the Sc-GAP.

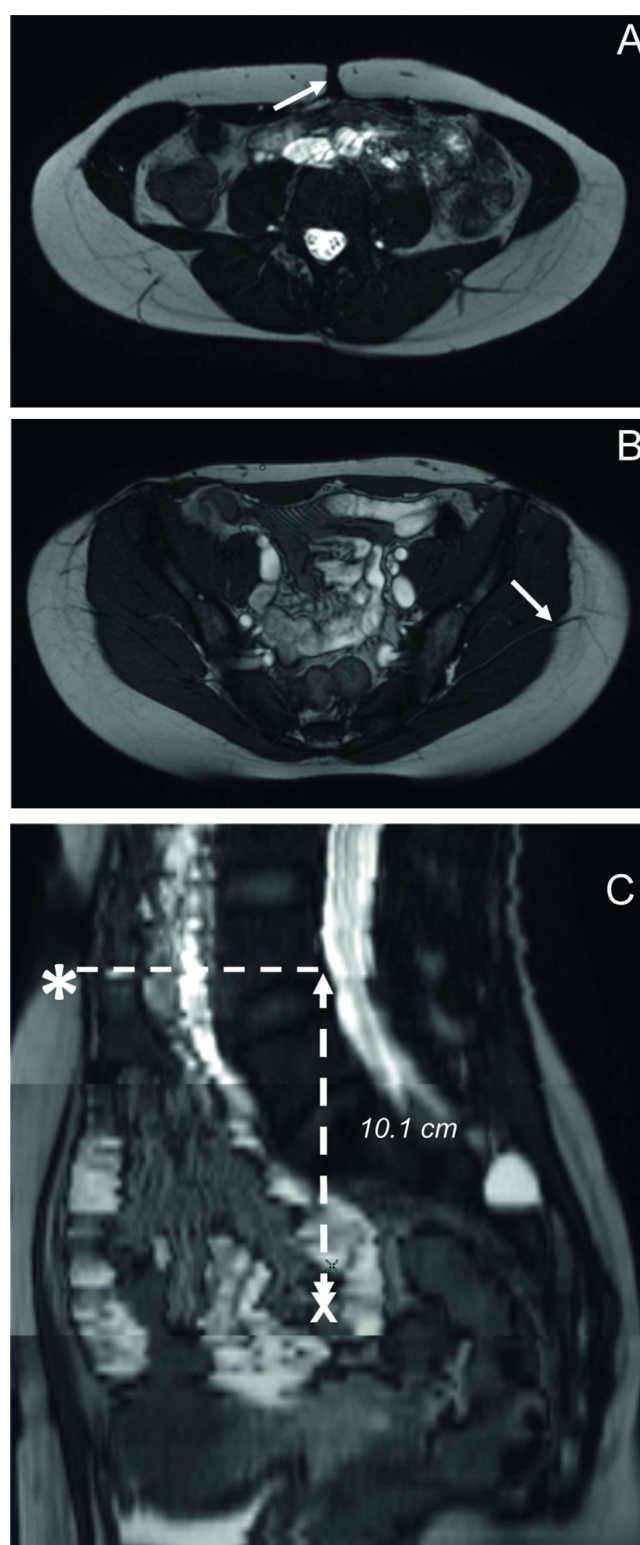


Figure 8. An example of how to assess the anteroposterior length. Firstly, the location of umbilicus is determined (A, arrow). Secondly, the location of the exit of the perforator between the gluteal muscles into the subcutaneous fat is determined (B, arrow). Finally, the position of the umbilicus, determined on the sagittal reconstructed images (C, asterisk), and the site of the perforator exit of B are marked by the crosshair (C, arrow). In this way, the craniocaudal length from the umbilicus to the site of the perforator exit can be determined. It was 10.1 cm in this example.

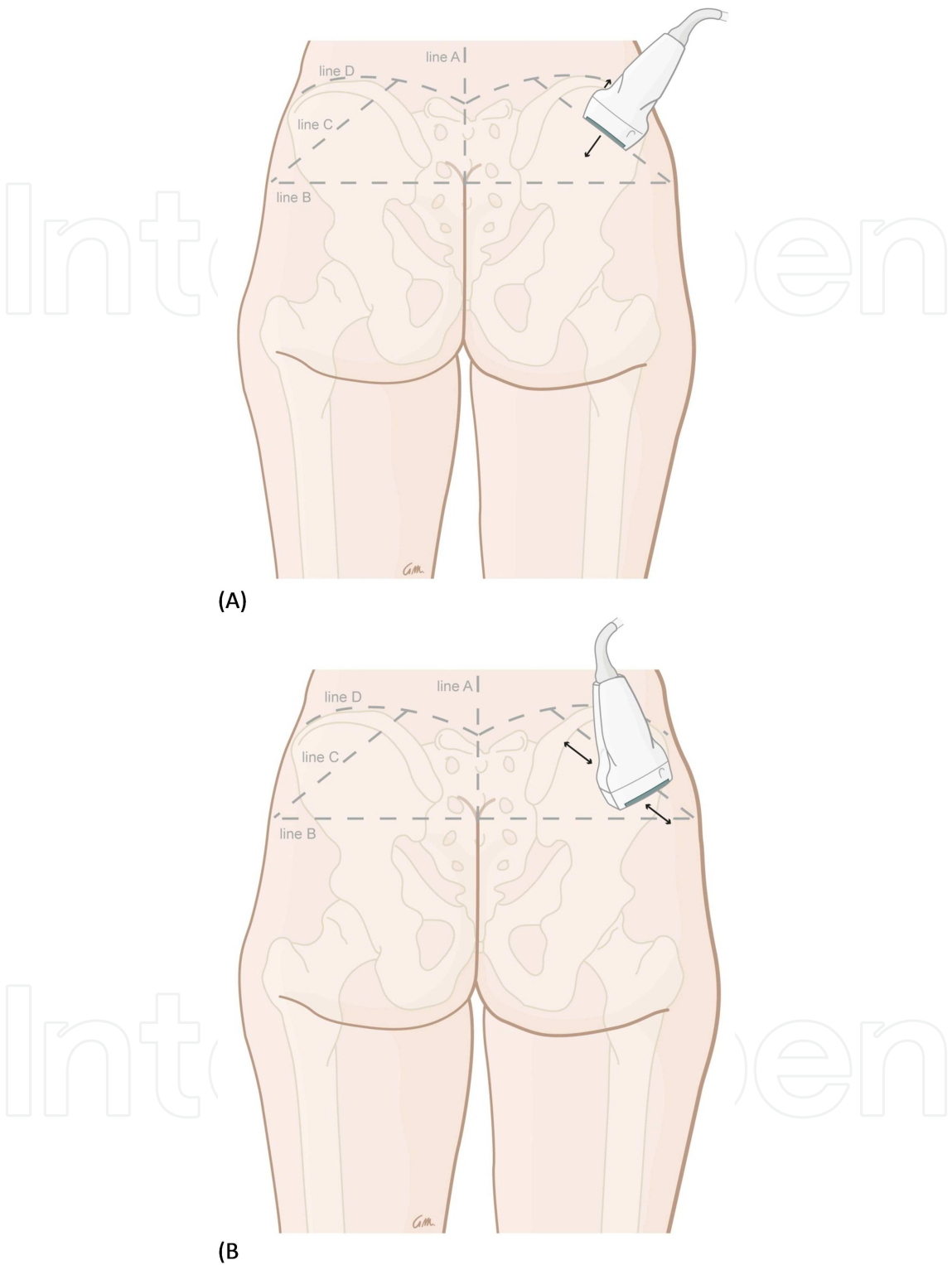


Figure 9. Schematic illustration of the identification of the cranial margin of the gluteus maximus muscle. line A: mid-line, line B: cranial end of the crena analis, line C: cranial border of m. gluteus maximus, line D: iliac crest. (A): probe positioned parallel to the margin of the gluteus maximus. (B): probe rotated 90 degrees and positioned perpendicularly to the margin of the gluteus maximus to identify the perforators. Illustration of Greet Mommen, www.greet-mommen.be.

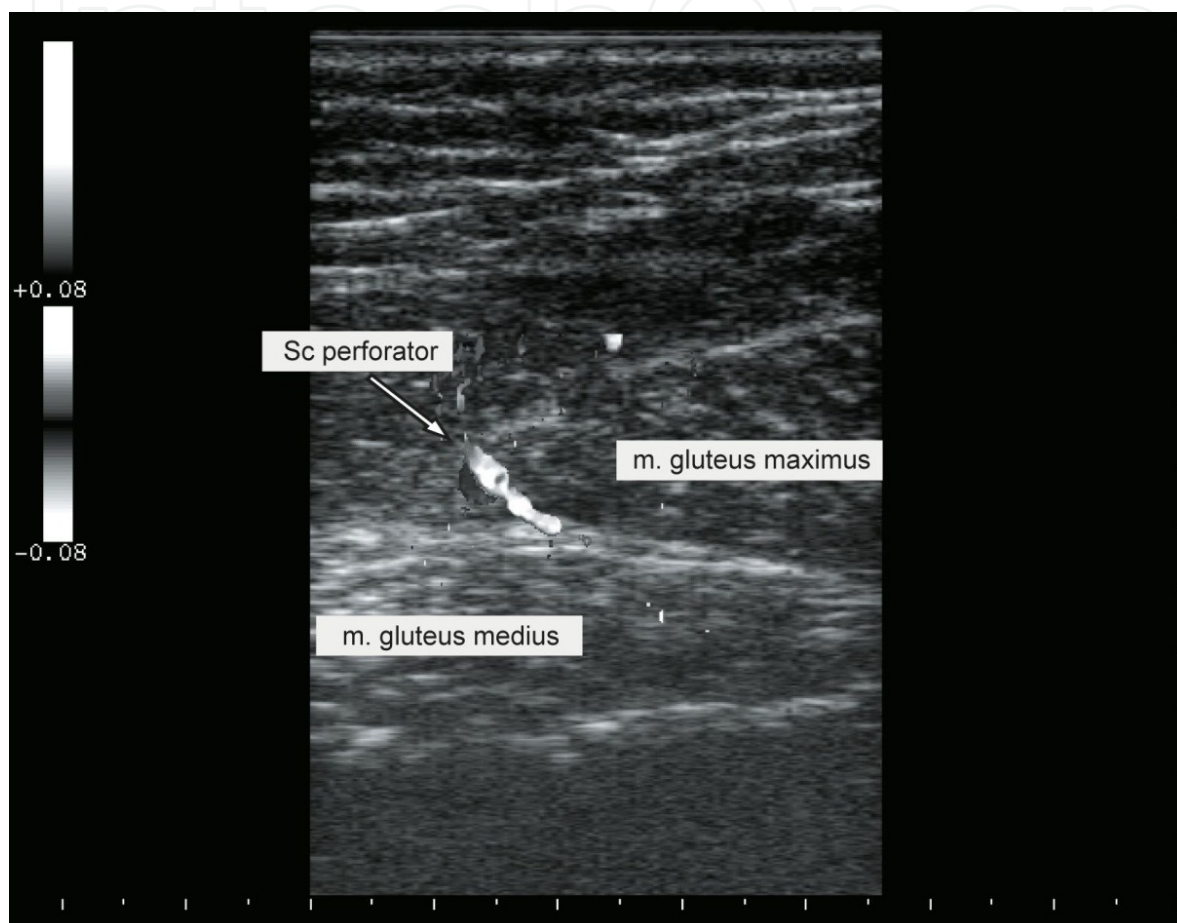


Figure 10. Visualization with Color Doppler of a perforator emerging between gluteus maximus and medius muscles.

Step 4: Adding all this information enables a precise identification of the perforator with the preferred location and length. In our first cases the flap contour, centered on this perforator, was always drawn elliptically completely on the superficial projection of the intermuscular septum between gluteus maximus and medius muscle. This ensures that, when marking proves not to be exact enough or the perforator chosen at first instance is damaged, alternative septocutaneous perforators, if present, can be used as pedicle for the flap. Out of experience the elliptical skin island now is changed in an S-shape to avoid undesirable dog ears medially and laterally (fig 11A, B).

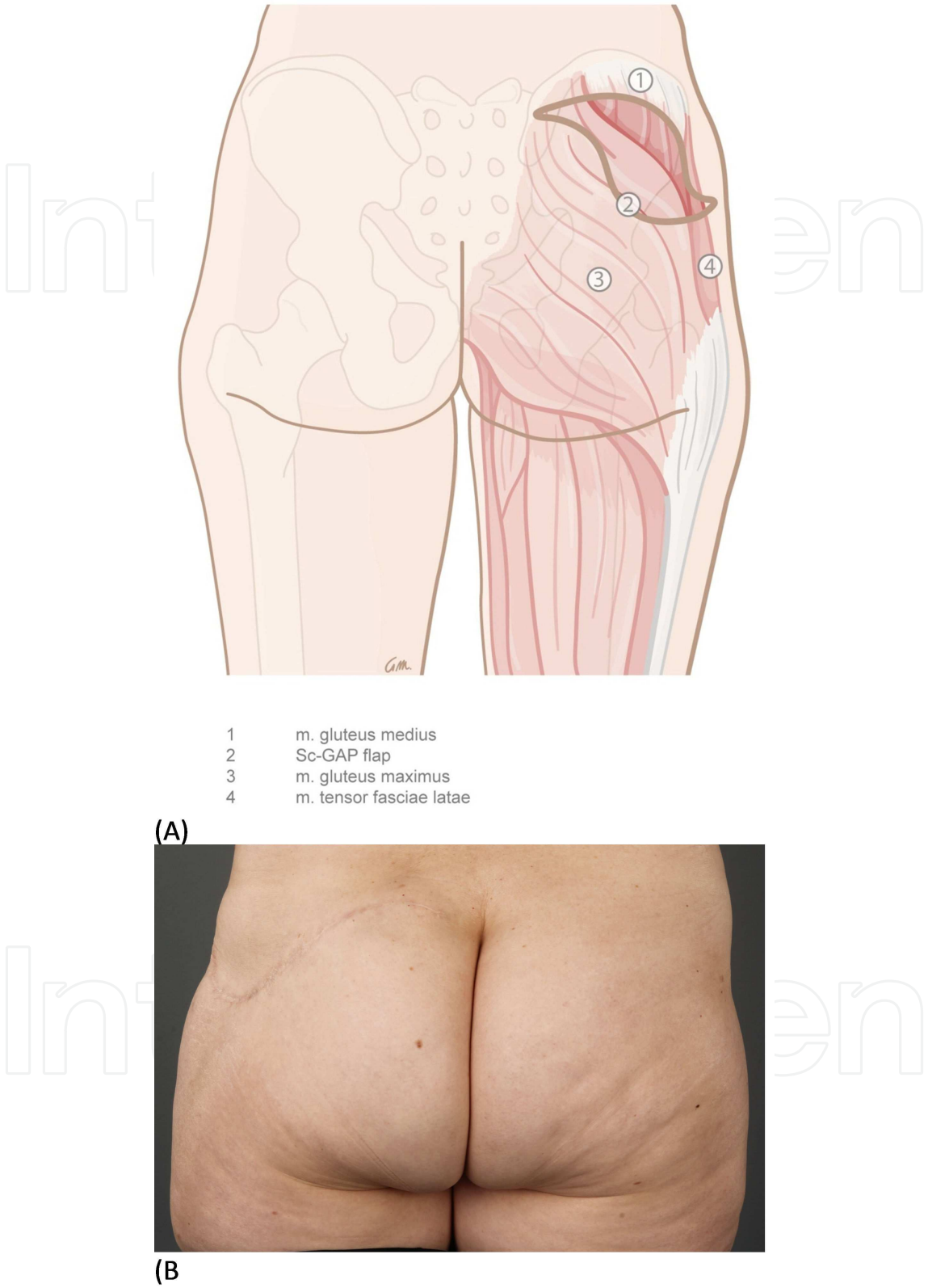


Figure 11. S-shaped design of the flap: (A) schematic visualization. (B) example on a patient. Illustration of Greet Mommen, www.greetmommen.be.

The pinch test is used to identify the maximal width of the flap. The flap is just orientated a bit more cranial than the standard drawing of an S-GAP flap (fig 12).

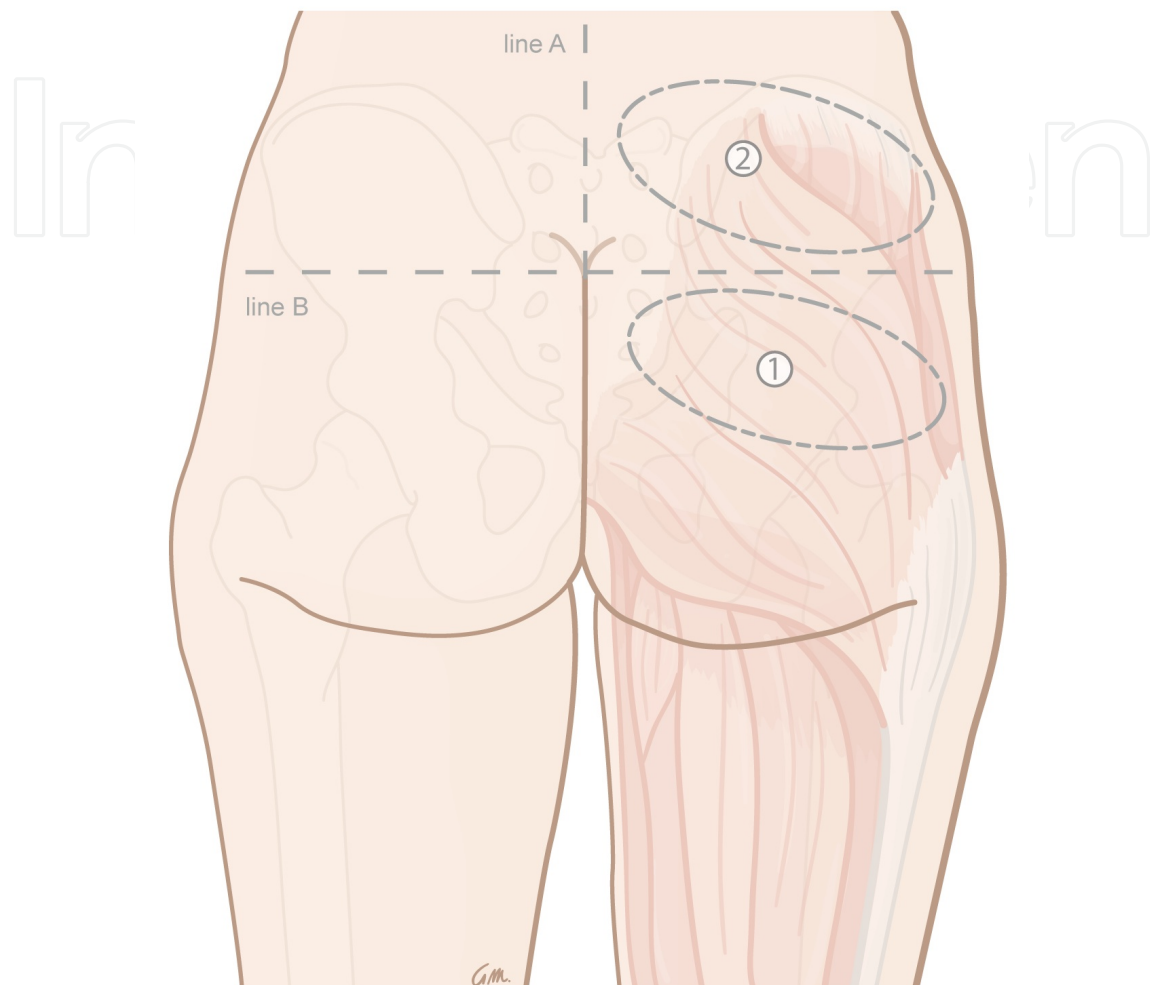


Figure 12. Schematic illustration of (1) region where a standard S-GAP is usually drawn and (2) region where the Sc-GAP is drawn. Illustration of Greet Mommen, www.greetmommen.be.

4. Surgical technique

The patient is initially supine. The internal mammary (thoracic) vessels are identified first, to reduce the ischemic time of the flap later on, especially in bilateral reconstructions.

The patient then is turned in prone position. The dissection starts at the craniomedial (fig 13), thin origin of the gluteus maximus muscle. Medially is the best starting point because perforators 6-8 cm from the midline, being too short, are not suitable as pedicle for the flap. The craniomedial edge of the gluteus maximus is identified and the fascia is opened.

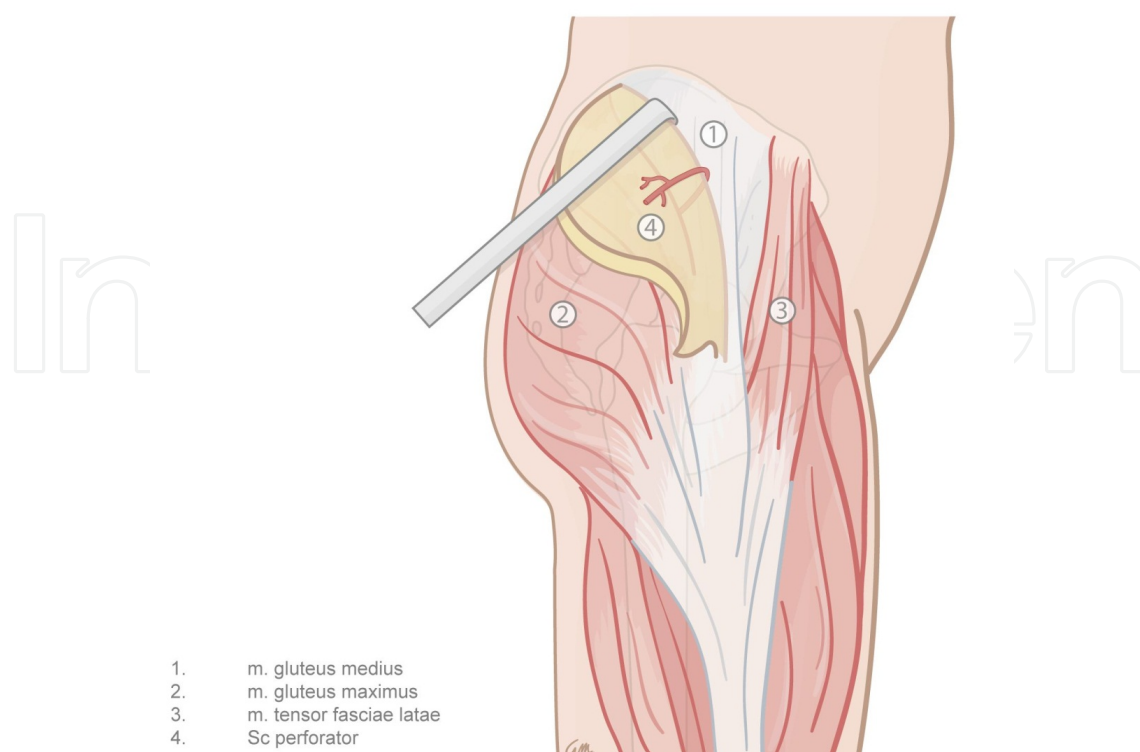
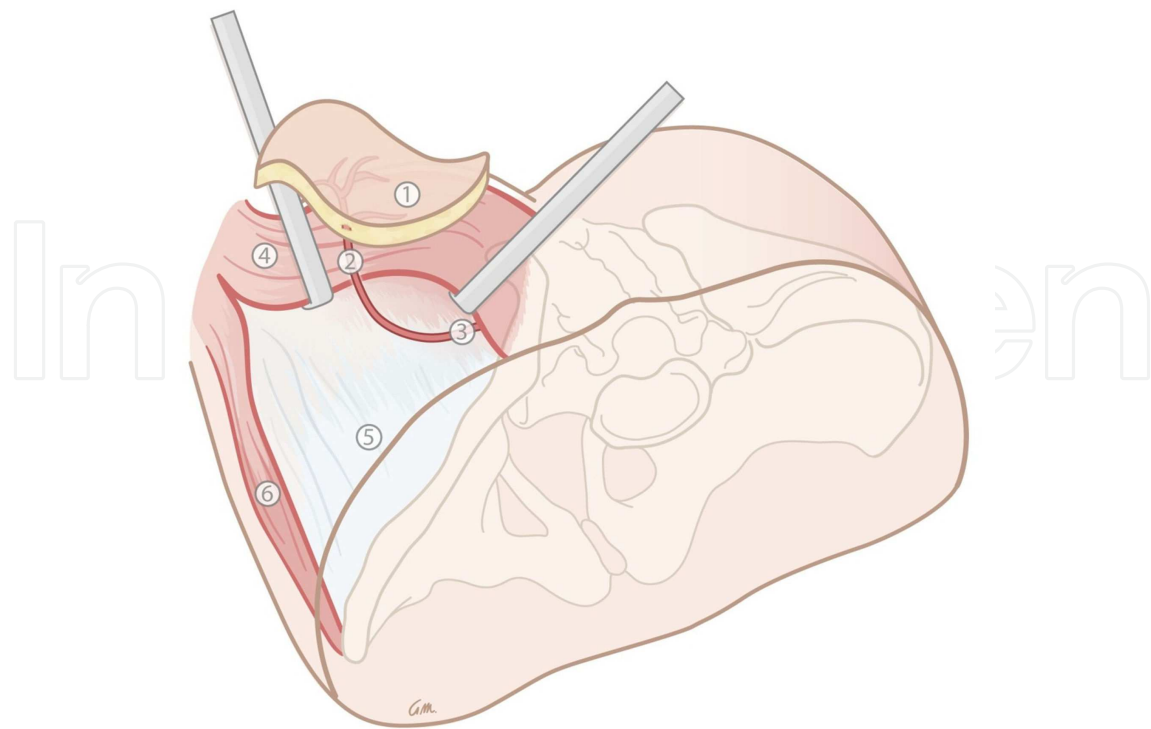


Figure 13. Craniomedial dissection of the Sc-GAP flap. Illustration of Greet Mommen, www.greetmommen.be.

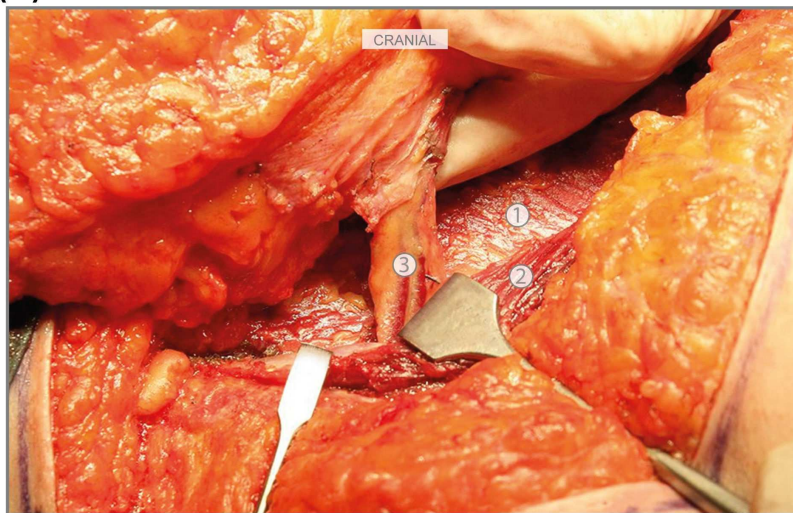
Actually, underneath the thin medial origin of the gluteus maximus muscle, it is very easy to develop in a blunt way a dissectional plane between the gluteus maximus and medius muscles and, introducing the finger into this plane, sometimes the pulsation of the perforator can be felt: this offers the opportunity to identify the exact location where the perforator emerges from the tight cranial fascial border between the gluteus maximus and medius muscles. The dissection continues in a retrograde way from medial to lateral, paying attention not to damage perforators emerging from the septum between the gluteus maximus and medius. The fascia of the gluteal muscles is very tight in this region and the approach of the septal plane between the gluteus maximus and medius is sometimes not easy: therefore this approach is a key point in the dissection. When the perforator(s) are identified the complete flap is incised and isolated.

The dissection continues, lifting the gluteus maximus muscle (fig 14 A, B) with the aid of a light hook. When the muscle is very tight it is difficult to lift it enough. In that case the gluteus maximus can partially be dissected at its origin on the sacrum and later on be sutured back. The perforator is followed between the gluteus maximus and medius paying attention to ligate every muscular or musculocutaneous branch. In the intermuscular septal plane the perforators join the superficial branch of the SGA (see anatomy). Near the sacrum the perforator continues retrogradely, running deep from the gluteus medius to reach its origin at the SGA. There the caput medusae of veins is present. These veins have usually a caliber above the 3 mm and are very fragile, having a very thin wall. To avoid problems the dissection is finished just before the caput medusae.



1. Sc-GAP flap
2. Sc perforator
3. SGA: superficial branch
4. m. gluteus maximus
5. m. gluteus medius
6. m. tensor fascia latae

(A)



1. m. gluteus medius
2. cranial border m. gluteus maximus
3. Sc perforator

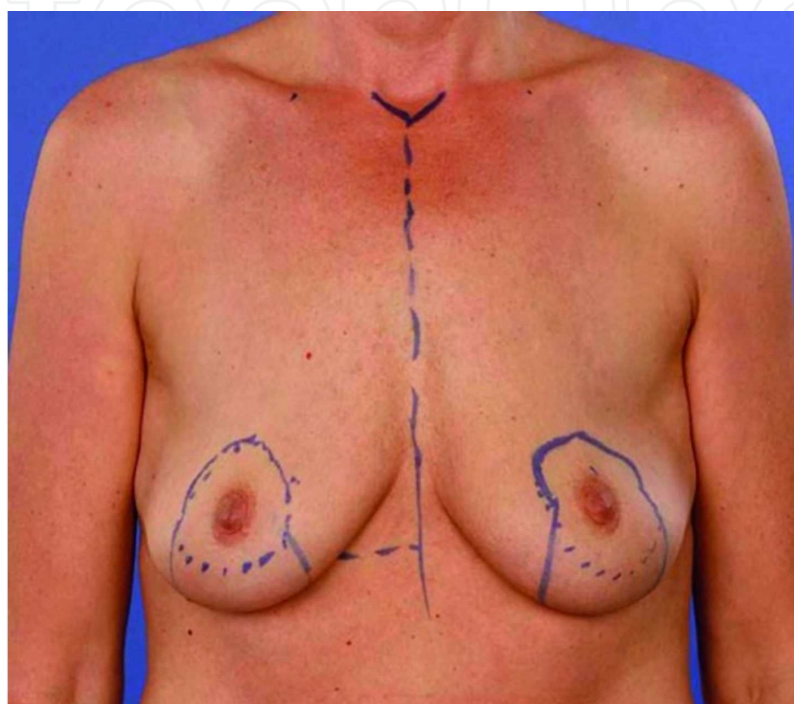
(B)

Figure 14. Musculus gluteus maximus lifted up, showing interseptal course of septocutaneous perforator, (A) schematic illustration and (B) intraoperative finding. Illustration of Greet Mommen, www.greetmommen.be.

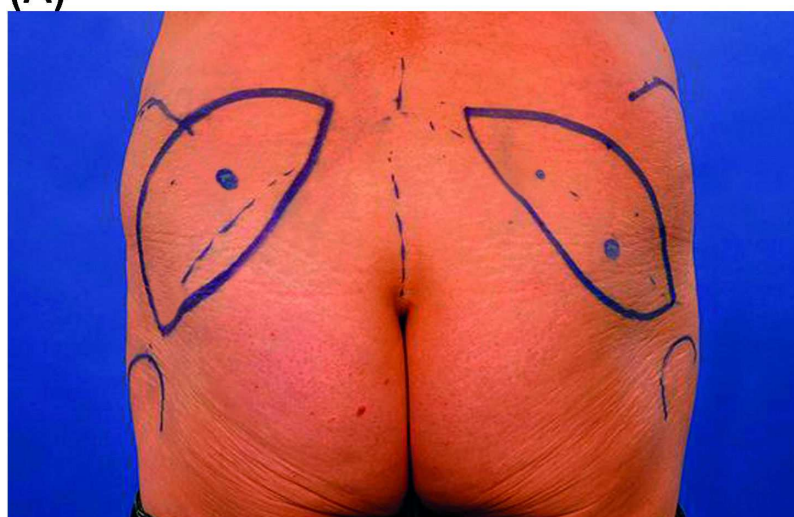
The flap is then removed from the gluteal region and the ischemia time starts. The donor site is closed, 2 drains are positioned and the patient is turned in supine position.

The anastomosis to the internal mammary (thoracic) vessels proceeds in the same way as for a DIEP flap.

Some preoperative pictures (fig 15 A, B) and postoperative results (fig 16 A, B) are shown.



(A)

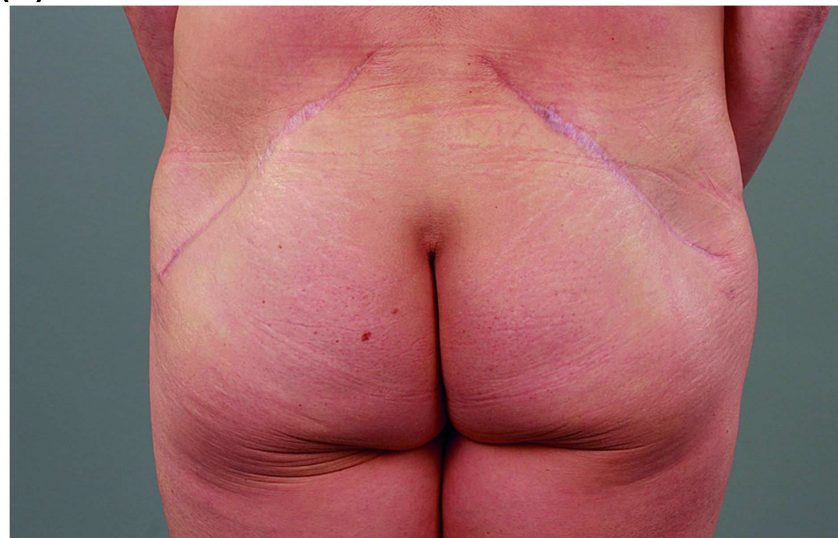


(B)

Figure 15. Preoperative pictures of (A) breasts and (B) gluteal region: bony landmarks and drawing of the flaps with perforators at the cranial border of the gluteus maximus muscle are visible.



(A)



(B)

Figure 16. Postoperative pictures of (A) breasts and (B) gluteal region.

5. Pitfalls

1. Do not consider suitable for surgery a perforator with a pedicle length measured on MRA less than 6 cm: the anastomosis with the mammary vessels will be very difficult.
2. Draw your patient in the exact same position as she will have during the operation (in our practice patients will have a pillow underneath the abdomen in the operative theatre): the skin of the gluteal region can move very easily with respect to the muscles because of the presence of a lot of subcutaneous tissue. A different position during drawing and operation can lead to a shift in the position of the septal plane and the perforator.

3. The identification of the septal plane between the gluteus maximus and medius muscles is essential: actually it is the key point of the dissection.
4. Lift the gluteus maximus muscle carefully because you can damage muscular or musculocutaneous branches of the superficial branch of the SGA.
5. If a clear visualization of the perforator is not possible, the gluteus maximus can partially detached from his origin from the sacral bone and at the end be reattached.
6. To be sure to include the perforator, chosen with the MRA, the flap is oriented just cranial to the edge of the gluteus maximus muscle: getting more experienced in the exact identification of the perforator offers the opportunity to change the flap orientation to improve aesthetic results. Because of the large number of perforators in this area it is not difficult to identify one of them with a standard Doppler, but you still don't know if it is a septocutaneous or a musculocutaneous one. The dissection especially will be very difficult when you accidentally have chosen a musculocutaneous perforator running into the gluteus medius muscles (see fig 3).
7. Septocutaneous perforators, compared to musculocutaneous ones, are surrounded by a greater amount of fat and connective tissue. Therefore they are more compact than musculocutaneous ones and, as a consequence, less flexible: the plastic surgeon has to pay more attention to maintain the original orientation of the pedicle to avoid torsion or kinking during positioning of the flap on the breast. The orientation can be maintained visually by marking the upper surface of the pedicle with ink.

Acknowledgements

We would like to give special thanks to Greet Mommen, medical scientific illustrator at Maastricht University, Department of Anatomy and Embryology, for the realization of the illustrations in this chapter. Her ideas and active contribution were essential to make clear the concepts, described above.

Author details

Stefania Tuinder^{1*}, Rene Van Der Hulst¹, Marc Lobbes², Bas Versluis² and Arno Lataster³

*Address all correspondence to: nervofaciale@yahoo.it

1 Department of Plastic and Reconstructive Surgery, MUMC+, Maastricht, The Netherlands

2 Department of Radiology, MUMC++, Maastricht, The Netherlands

3 Department of Anatomy & Embryology, Maastricht University, Maastricht, The Netherlands

References

- [1] Fujino, T, Harashina, T, & Enomoto, K. Primary breast reconstruction after a standard radical mastectomy by a free flap transfer (case report). *Plast Reconstr Surg.* (1976). , 58(3), 371-4.
- [2] Shaw, W. W. Breast reconstruction by superior gluteal microvascular free flaps without silicone implants. *Plast Reconstr Surg.* (1983). , 72(4), 490-501.
- [3] Allen, R. Tucker C Jr. Superior gluteal artery perforator free flap for breast reconstruction. *Plast Reconstr Surg.* (1995). , 95(7), 1207-12.
- [4] LoTempio MMAllen RJ. Breast reconstruction with SGAP and IGAP flaps. *Plast Reconstr Surg.* (2010). Review., 126(2), 393-401.
- [5] Koshima, I, Moriguchi, T, Fukuda, H, Yoshikawa, Y, & Soeda, S. Free, thinned, parambilical perforator-based flaps. *J Reconstr Microsurg.* (1991). , 7(4), 313-6.
- [6] Allen, R. J, & Treece, P. Deep inferior epigastric perforator flap for breast reconstruction. *Ann Plast Surg.* (1994). , 32(1), 32-8.
- [7] Blondeel, P. N, Van Landuyt, K. H, Monstrey, S. J, Hamdi, M, Matton, G. E, Allen, R. J, Dupin, C, Feller, A. M, Koshima, I, Kostakoglu, N, & Wei, F. C. The "Gent" consensus on perforator flap terminology: preliminary definitions. *Plast Reconstr Surg.* (2003). quiz 1383, 1516; discussion 1384-7., 112(5), 1378-83.
- [8] Geddes, C. R, Morris, S. F, & Neligan, P. C. Perforator flaps: evolution, classification and application. *Ann Plast Surg* (2003). Review., 50(1), 90-9.
- [9] Blondeel, P. N, Morris, S. F, Hallock, G. G, & Neligan, P. C. eds. *Perforator flaps: Anatomy, Technique and Clinical Application*. St. Louis: Quality Medical; (2006).
- [10] Sinna, R, Boloorch, A, Mahajan, A. L, Qassemyar, Q, & Robbe, M. What should define a "perforator flap"? *Plast Reconstr Surg.* (2010). Review., 126(6), 2258-63.
- [11] Taylor, G. I, Rozen, W. M, & Whitaker, I. S. Establishing a perforator flap nomenclature based on anatomical principles. *Plast Reconstr Surg.* (2012). e-9e.
- [12] Tuinder, S, Van Der Hulst, R, Lataster, A, & Boeckx, W. Superior gluteal artery perforator flap based on septal perforators: preliminary study. *Plast Reconstr Surg.* (2008). e-8e.
- [13] Tuinder, S, Chen, C. M, & Massey, M. F. Allen RJ Sr, Van der Hulst R. Introducing the septocutaneous gluteal artery perforator flap: a simplified approach to microsurgical breast reconstruction. *Plast Reconstr Surg.* (2011). , 127(2), 489-95.
- [14] Warwick, R, & Williams, P. L. (1973). *Gray's Anatomy*, 35th Edition, Edinburgh: Longman Group Ltd.

- [15] Moore, K. L. (1992). *Clinically Oriented Anatomy*, 3rd Edition, Baltimore: Williams & Wilkins.
- [16] Stone, R. J, & Stone, J. A. (2000). *Atlas of Skeletal Muscles*, 3rd Edition, Boston: McGraw- Hill Companies Inc.
- [17] Cormack, G. C, & Lamberty, B. G. H. (1994). *The Arterial Anatomy of Skin Flaps*, 2nd Ed. New York: Churchill Livingstone;, 218-22.
- [18] Mathes, D. W, & Neligan, P. C. Current techniques in preoperative imaging for abdomen-based perforator flap microsurgical breast reconstruction. *J Reconstr Microsurg.* (2010). , 26(1), 3-10.
- [19] Chernyak, V, Rozenblit, A. M, Greenspun, D. T, et al. Breast reconstruction with deep inferior epigastric artery perforator flap: 3.0-T gadolinium-enhanced MR imaging for preoperative localization of abdominal wall perforators. *Radiology.* (2009). , 250(2), 417-24.
- [20] Rozen, W. M, Phillips, T. J, Ashton, M. W, et al. Preoperative imaging for DIEA perforator flaps: a comparative study of computed tomographic angiography and Doppler ultrasound. *Plast Reconstr Surg.* (2008). , 121(1), 9-16.
- [21] Alonso-burgos, A, Garcia-tutor, E, Bastarrika, G, et al. Preoperative planning of deep inferior epigastric artery perforator flap reconstruction with multislice-CT angiography: imaging findings and initial experience. *J Plast Reconstr Aesthet Surg.* (2006). , 59(6), 585-93.
- [22] Masia, J, Clavero, J. A, Larranaga, J. R, et al. Multidetector-row computed tomography in the planning of abdominal perforator flaps. *J Plast Reconstr Aesthet Surg.* (2006). , 59(6), 594-9.
- [23] Acosta, R, Smit, J. M, Audolfsson, T, et al. A Clinical Review of 9 Years of Free Perforator Flap Breast Reconstructions: An Analysis of 675 Flaps and the Influence of New Techniques on Clinical Practice. *J Reconstr Microsurg.* (2011). Feb;; 27(2), 91-8.
- [24] Giunta, R. E, Geisweid, A, & Feller, A. M. The value of preoperative Doppler sonography for planning free perforator flaps. *Plast Reconstr Surg.* (2000). , 105(7), 2381-6.
- [25] Brenner, D. J, Doll, R, Goodhead, D. T, et al. Cancer risks attributable to low doses of ionizing radiation: assessing what we really know. *Proc Natl Acad Sci U S A.* (2003). , 100(24), 13761-6.
- [26] Hall, E. J, & Brenner, D. J. Cancer risks from diagnostic radiology. *Br J Radiol.* (2008). , 81(965), 362-78.
- [27] Einstein, A. J. Medical imaging: the radiation issue. *Nat Rev Cardiol.* (2009). , 6(6), 436-8.
- [28] Rozen, W. M, Stella, D. L, Phillips, T. J, et al. Magnetic resonance angiography in the preoperative planning of DIEA perforator flaps. *Plast Reconstr Surg.* (2008). e-3e.
- [29] Fukaya, E, Grossman, R. F, Saloner, D, et al. Magnetic resonance angiography for free fibula flap transfer. *J Reconstr Microsurg.* (2007). , 23(4), 205-11.